

Orientation dependence in multichannel dissociative ionization of OCS molecules

Yusuke Sakemi,¹ Shinichirou Minemoto,¹ and Hirofumi Sakai^{1,2,*}

¹*Department of Physics, Graduate School of Science, The University of Tokyo, 7-3-1 Hongo, Bunkyo-ku, Tokyo 113-0033, Japan*

²*Institute for Photon Science and Technology, Graduate School of Science, The University of Tokyo, 7-3-1 Hongo, Bunkyo-ku, Tokyo 113-0033, Japan*

(Received 7 October 2016; published 11 July 2017)

With 800-nm, 25-fs elliptically polarized ionization pulses, we observe molecular frame photoelectron angular distributions (MF-PADs) correlated with different dissociative ionization channels: $\text{OCS}^+ \rightarrow \text{S}^+ + \text{CO}$, $\text{CO}^+ + \text{S}$, $\text{CS}^+ + \text{O}$, and $\text{O}^+ + \text{CS}$. We find that the asymmetry in the MF-PAD depends on the specific dissociation channel and the laser intensities. For the dissociation channel leading to the production of O^+ , the OCS molecules are more likely to be ionized when the electric field points toward the O atom, while for other dissociation channels, they are more likely to be ionized when the electric field points toward the S atom.

DOI: [10.1103/PhysRevA.96.011401](https://doi.org/10.1103/PhysRevA.96.011401)

Tunnel ionization in atoms and molecules is a basic process in high-order harmonic generation (HHG) [1,2], above-threshold ionization (ATI) [3], laser-induced photoelectron diffraction [4], and nonsequential double ionization [5]. For small symmetric nonpolar molecules such as N_2 , O_2 , and CO_2 , angle-dependent ionization rates are successfully predicted by the molecular-orbital Ammosov-Delone-Krainov (MO-ADK) model [6]. In general, the angular dependence of the ionization rate reflects the shape of the highest occupied molecular orbital (HOMO) of the molecule [7]. However, in the case of asymmetric polar molecules, it is not easy to predict the angular dependence of the ionization rate. For example, the MO-ADK model predicts that OCS molecules are more likely to be ionized when the electric field points toward the O atom than when it points toward the S atom, which is not consistent with the experimental result reported in Ref. [8], where the orientation dependence of the ionization rate is investigated by using a sample of oriented molecules in the presence of an intense laser field. The observation reported in Ref. [8] is explained by an extended tunneling model in which the laser-induced Stark shifts associated with the dipoles and polarizabilities of the molecule and its cation are taken into account [9,10]. Some groups are also trying to construct appropriate tunneling models [11–13] to predict photoelectron angular distributions from polar molecules ionized by intense femtosecond pulses.

In addition to tunnel ionization, molecules can dissociate into fragment ions if the produced molecular cations are prepared in vibrational levels which cannot be supported by molecular ionic states after tunnel ionization. Here we investigate orientation dependence in dissociative tunnel ionization of OCS molecules. The present study consists of the following two steps: (1) We observe molecular frame photoelectron angular distributions, which we call MF-PADs, of OCS molecules by doing the coincidence measurements between the fragment ions and photoelectrons. (2) Then we reveal the correlation between the orientation dependence of ionization and the specific dissociative ionization channel. The orientation dependence in laser tunnel ionization from multiple orbitals in diatomic HCl molecules was investigated by using

a similar experimental technique [14]. In contrast, we report the experimental study on orientation dependence in the *multichannel* dissociative ionization of *triatomic* OCS molecules. In the case of triatomic molecules, their cations can dissociate into some different dissociation channels. Specifically, OCS^+ ion can dissociate into $\text{S}^+ + \text{CO}$, $\text{CO}^+ + \text{S}$, $\text{CS}^+ + \text{O}$, and $\text{O}^+ + \text{CS}$. Obviously, it is much more advantageous for us to discriminate a specific dissociation channel from other channels to obtain more detailed information about the orientation dependence of ionization rate in triatomic molecules. Then based on the observed results, we discuss the tunnel ionization dynamics of OCS molecules. As for the theory of *dissociative* tunnel ionization, we find that the first work was recently reported with analytic expressions for the nuclear kinetic energy distribution of the ionization rates [15]. In Ref. [15], although the nuclear kinetic energy release (KER) spectrum and the way to image the field-dressed nuclear wave function from the KER spectrum are mainly discussed for the simplest molecular ion H_2^+ as an example, nothing has been discussed about alignment dependence in dissociative tunnel ionization of H_2^+ . Therefore, we emphasize that there is no existing tunneling model which can be used to predict photoelectron angular distributions from OCS molecules depending on a specific dissociative ionization channel.

To observe MF-PADs, we employ the angular streaking method [16,17], where a circular polarization or an elliptical polarization with higher ellipticity is used for an ionization pulse. Then the final drift velocity of the ionized electron is determined by the vector potential at the instant of the ionization. Suppose that the actual angle-dependent ionization rate of a sample molecule looks as in Fig. 1(b) at the instant of ionization. When the molecules are irradiated with the left circularly polarized pulse [drawn as counterclockwise (CCW) in Fig. 1], the photoelectron angular distribution should look as in Fig. 1(a). On the other hand, when the molecules are irradiated with the right circularly polarized pulse [drawn as clockwise (CW) in Fig. 1], the photoelectron angular distribution should look as in Fig. 1(c). Consequently, MF-PADs reflect the orientation dependence of tunnel ionization in the sample molecule. The opposite photoelectron angular distributions obtained with left and right circularly polarized pulses can be used to ensure the validity of the observed results.

*hsakai@phys.s.u-tokyo.ac.jp

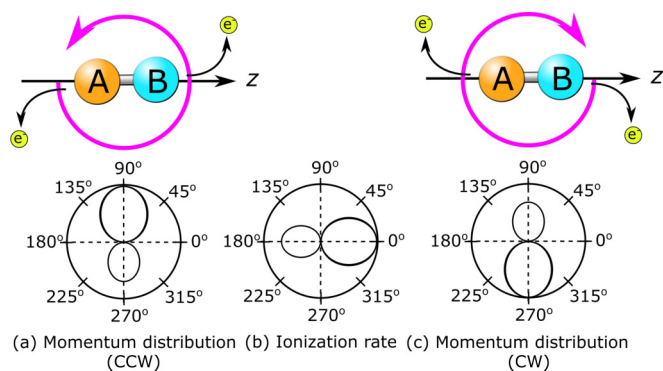


FIG. 1. Principle of the angular streaking method. Suppose that the actual angle-dependent ionization rate of a sample molecule looks as in (b) at the instant of ionization. When the molecules are irradiated with the left circularly polarized pulse [drawn as counterclockwise (CCW)], the photoelectron angular distribution should look as in (a). On the other hand, when the molecules are irradiated with the right circularly polarized pulse [drawn as clockwise (CW)], the photoelectron angular distribution should look as in (c).

As an ionization pulse, we use the output from a Ti:sapphire based chirped pulse amplification system (FEMTOLASERS Produktions GmbH, FEMTOPOWER PRO V CEP) with the center wavelength of ~ 800 nm and the pulse width of ~ 25 fs. The intensity of the ionization pulse is controlled by the combination of a half-wave plate and a thin film polarizer. On the other hand, the ellipticity of the ionization pulse is controlled by rotating a half-wave plate placed before the quarter-wave plate. Thereby we prepare both clockwise and counterclockwise elliptical polarizations with the ellipticity of 0.84.

To make coincidence measurements, a coincidence velocity map imaging spectrometer, which we call a CO-VIS apparatus, was developed in our group and its basic design is similar to that reported in Ref. [18]. The schematic diagram of the CO-VIS apparatus is shown in Fig. 2(a). The CO-VIS apparatus consists of three chambers, i.e., the source chamber, the differential pumping chamber, and the main chamber. The sample gas is supplied by an Even-Lavie valve [19] equipped in the source chamber. The femtosecond ionization pulse is focused by a 100-mm-focal-length concave mirror located in the main chamber, in which two time-and-position sensitive

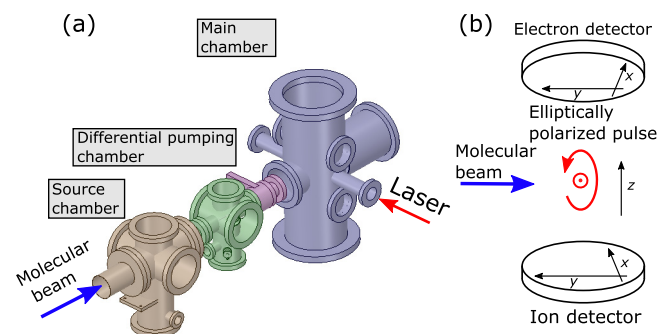


FIG. 2. (a) Schematic diagram of a coincidence velocity map imaging spectrometer (CO-VIS) apparatus. (b) Coordinate system to be used in data analysis.

detectors are equipped face to face. The upper detector is used to detect photoelectrons and the lower one is used to detect fragment ions. The coordinate system to be used in data analysis is defined in Fig. 2(b). The molecular beam propagates along the y axis and the time-of-flight (TOF) axis is parallel to the z axis. By utilizing the elliptical polarization with its major axis parallel to the z axis, we can determine the direction of the sample molecules which dominantly contribute to the observed momentum distributions of the fragment ions. This approach is essential in the CO-VIS measurements to obtain the laboratory-frame photoelectron angular distributions and to further transform them into the MF-PADs. This is because the time resolution for photoelectrons is not high enough in the CO-VIS measurements to obtain the so-called three-dimensional momentum distributions of photoelectrons in contrast to the COLTRIMS (cold target recoil ion momentum spectrometer) measurements [14,16,17].

Figure 3(a) shows a typical momentum distribution of CO^+ fragment ions. The horizontal axis represents the momentum along the z axis and the vertical axis represents the momentum along the y axis. The strong signal near the center comes from N_2^+ ions, which are one of the dominant background molecules in the vacuum chamber and its mass-to-charge ratio ($A/q = 28$) is the same as that of CO^+ . However, since the molecular beam propagates downward in the momentum distribution shown in Fig. 3(a), the signals of the CO^+ fragment ions are shifted downward according to the velocity of the molecular beam, which is estimated to be about 400 m/s. A pair of CO^+ ions with smaller momenta comes from the dissociation channel. That is, OCS^+ ions dissociate into CO^+ and neutral S. On the other hand, a pair of CO^+ ions with larger momenta comes from the Coulomb explosion. That is, OCS^{2+} dications dissociate into CO^+ and S^+ . Although the CO^+ ions are successfully discriminated from the background N_2^+ ions because of the velocity of the molecular beam, strictly speaking, the momentum distribution of CO^+ and that of N_2^+ are not completely separated as shown in Fig. 3(a). To avoid the effect of the incompleteness in the separation of the momentum distributions between the two kinds of ions, we use the CO^+ ions produced from the OCS^+ cations within the vertex angle $\pi/2$ or $\pi/4$ as shown in Fig. 3(a) in the following analysis because those CO^+ ions are expected to be well separated from N_2^+ ions. The validity of this treatment for the fragment ions is discussed below.

Here we explain the procedure to obtain an MF-PAD. First, we observe both photoelectrons and (fragment) ions with the mass-to-charge ratios $A/q = 1$ (H^+ from background molecules such as H_2O) to 60 (OCS^+). Then we select a specific dissociation channel [e.g., $\text{OCS}^+ \rightarrow \text{CO}^+ + \text{S}$ as shown in Fig. 3(a)] for which its resultant fragment ions (CO^+) fly along the TOF axis, which is made possible by utilizing the elliptical polarization with its major axis along the z axis as explained above. By applying the coincidence condition, we can obtain an MF-PAD as shown in Fig. 3(b). In this MF-PAD, the horizontal axis represents the momentum along the x axis and the vertical axis represents the momentum along the y axis. The asymmetry in the momentum distribution shown in Fig. 3(b) shows the orientation dependence of tunnel ionization leading to the specific dissociation channel: $\text{OCS}^+ \rightarrow \text{CO}^+ + \text{S}$ as discussed below. As explained above, since the CO^+ ions

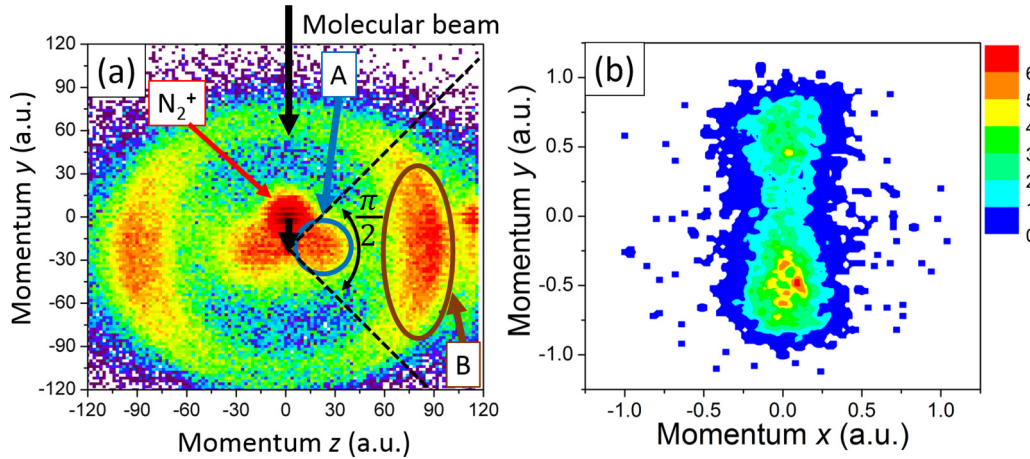


FIG. 3. (a) Typical momentum distribution of CO^+ fragment ions. The CO^+ ions labeled A are produced by the dissociation $\text{OCS}^+ \rightarrow \text{CO}^+ + \text{S}$, while those labeled B are produced by the Coulomb explosion $\text{OCS}^{2+} \rightarrow \text{CO}^+ + \text{S}^+$. In the data analysis, the CO^+ ions produced from the OCS^+ cations within the vertex angle $\pi/2$ or $\pi/4$ are used. In the figure, the vertex angle $\pi/2$ is shown. See text for the details. (b) An MF-PAD can be obtained by applying the coincidence condition. The photoelectrons are all correlated with the CO^+ ions produced from the OCS^+ cations within the vertex angle $\pi/2$.

produced from the OCS^+ cations within the vertex angle $\pi/2$ or $\pi/4$ as shown in Fig. 3(a) are used in the analysis, the photoelectrons shown in Fig. 3(b) are all correlated with those CO^+ ions.

Next we ensure the validity of our observations. Figure 4 shows MF-PADs obtained in different conditions all correlated with CO^+ fragment ions. The left panels are the MF-PADs when OCS molecules are along the z axis with their O atoms directed upward. On the other hand, the right panels are those when OCS molecules are along the z axis with their O atoms directed downward. The upper panels are the MF-PADs obtained with clockwise elliptical polarization while the lower panels are those obtained with counterclockwise elliptical polarization. One can see that the up-down asymmetry in an MF-PAD is reversed when one of the above two conditions, i.e., the direction of OCS molecules or the helicity of elliptical polarization, is reversed. Such a behavior in the MF-PADs is consistent with our expectations explained by using Fig. 1 and ensures the validity of our observations. Since those four MF-PADs shown in Fig. 4 are physically equivalent with each other, we can take an average for the up-down asymmetry in the photoelectron angular distributions leading to the specific dissociation channel: $\text{OCS}^+ \rightarrow \text{CO}^+ + \text{S}$.

To quantify the up-down asymmetry, $N_{\text{up}}/N_{\text{total}}$ with N_{up} the number of photoelectrons observed in the upper half of MF-PADs and N_{total} the total number of the photoelectrons concerned, by using a set of four MF-PADs as shown in Fig. 4, we introduce an asymmetry parameter $A_{\text{MF-PAD}}$ defined by the following equation:

$$A_{\text{MF-PAD}} = \frac{1}{4} \sum_{\text{pol, axis}} \sigma_{\text{pol}} \sigma_{\text{axis}} \left(0.5 - \frac{N_{\text{up}}}{N_{\text{total}}} \right), \quad (1)$$

where two parameters σ_{pol} and σ_{axis} are introduced to compensate for the inversion in the up-down asymmetry when the observation condition is reversed. That is, σ_{pol} is 1 (−1) for clockwise (counterclockwise) elliptical polarization. And σ_{axis} is 1 (−1) when the S atom points toward $+z$ ($-z$) direction.

As a consequence of these definitions, when the asymmetry parameter $A_{\text{MF-PAD}}$ is positive (negative), the OCS molecules are more likely to be ionized when the field points toward the S (O) atom. In other words, if we follow the tunnel ionization picture in the long-wavelength limit, when the asymmetry parameter $A_{\text{MF-PAD}}$ is positive (negative), the OCS molecules are more likely to be ionized from the O (S) site.

Figure 5 shows the summary of the degrees of asymmetry $A_{\text{MF-PAD}}$ in MF-PADs as a function of the intensity of the ionization pulse. As mentioned above, the asymmetry parameter is obtained by using the photoelectrons correlated with the fragment ions produced from the OCS^+ cations within the vertex angle $\pi/2$ or $\pi/4$ as shown in Fig. 3(a). The fact that the results obtained by using the photoelectrons correlated with the fragment ions within the vertex angles $\pi/2$ and $\pi/4$ are in good agreement with each other for specific dissociation channels ensures that the results are not influenced by the background ions such as N_2^+ . The asymmetry parameter $A_{\text{MF-PAD}}$ is positive for the dissociation channels leading to the production of the fragment ions S^+ , CO^+ , and CS^+ , while it is negative for the dissociation channel leading to the production of the fragment ions O^+ . Therefore, for the dissociation channel leading to the production of O^+ , the OCS molecules are more likely to be ionized when the electric field points toward the O atom, while for other dissociation channels, they are more likely to be ionized when the electric field points toward the S atom. As a general tendency, the degrees of asymmetry are small when the intensity of the ionization pulse is low. For the dissociation channel leading to the production of CS^+ , the degree of asymmetry saturates already at $1.0 \times 10^{14} \text{ W/cm}^2$ and starts to decrease at higher intensities. For other dissociation channels, the degrees of asymmetry saturate at around $1.5 \times 10^{14} \text{ W/cm}^2$ and start to decrease at higher intensities. The decrease in the degrees of asymmetry suggests the significant production of OCS dications at higher intensities.

We consider how the OCS^+ cations dissociate into the specific fragment ions. In order for the singly charged cations

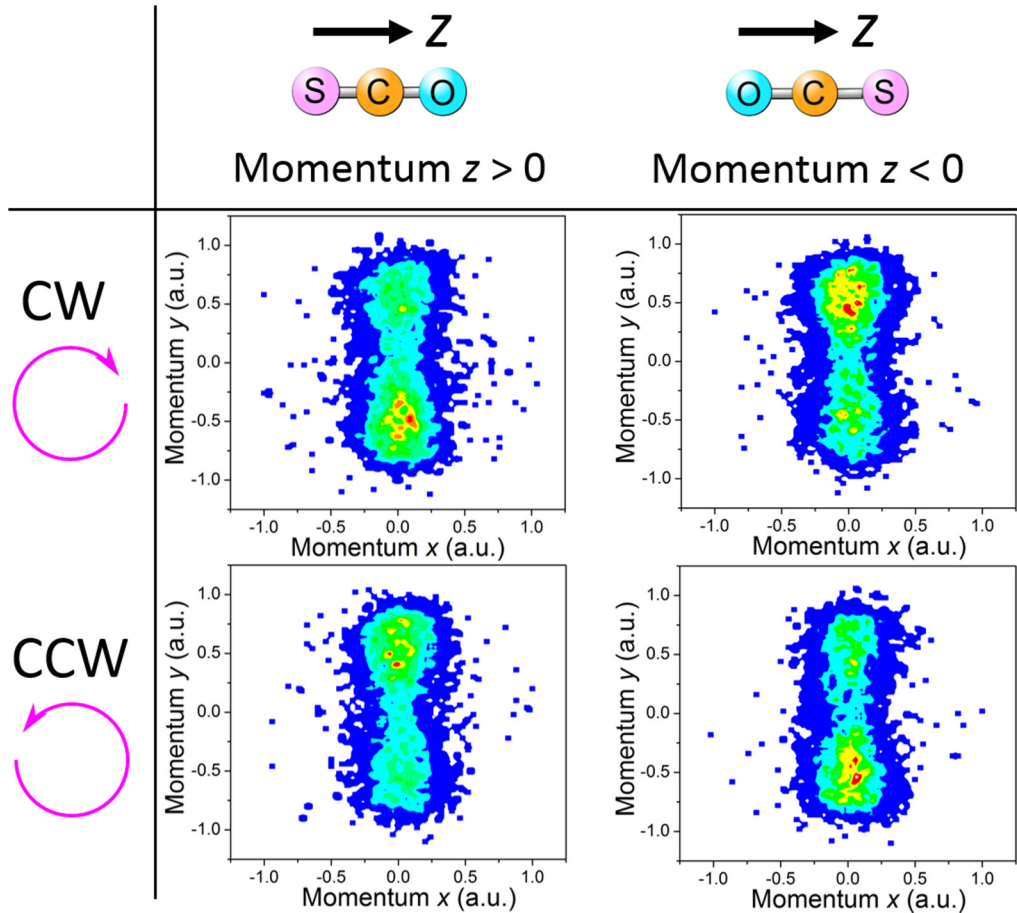


FIG. 4. MF-PADs obtained in different conditions all correlated with CO^+ fragment ions. The left panels are the MF-PADs when OCS molecules are along the z axis with their O atoms directed upward. The right panels are those when OCS molecules are along the z axis with their O atoms directed downward. The upper panels are the MF-PADs obtained with CW elliptical polarization while the lower panels are those obtained with CCW elliptical polarization. The color legend is shown in Fig. 3. In all the panels, the photoelectrons are all correlated with the CO^+ ions produced from the OCS^+ cations within the vertex angle $\pi/2$ as shown in Fig. 3(a).

to dissociate, the ions must be prepared on dissociative excited states. Here we consider the following three dissociation channels: $\text{OCS}^+ \rightarrow \text{S}^+ + \text{CO}$ (I), $\text{CO}^+ + \text{S}$ (II), and $\text{CS}^+ + \text{O}$ (III),

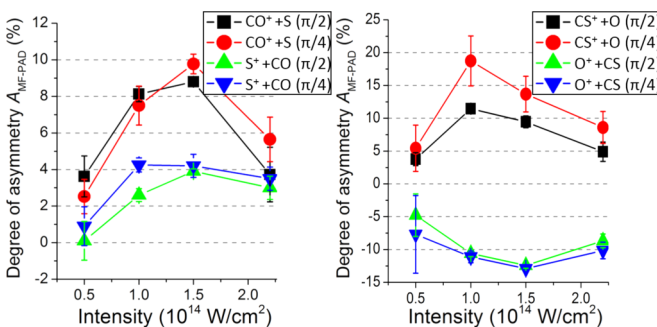


FIG. 5. Degrees of asymmetry $A_{\text{MF-PAD}}$ in MF-PADs as a function of the intensity of the ionization pulse for different dissociation channels. The specific dissociative ionization channels are shown in the legend. The asymmetry parameter is obtained by using the photoelectrons correlated with the fragment ions produced from the OCS^+ cations within the vertex angle $\pi/2$ or $\pi/4$ as shown in Fig. 3(a). The vertex angles are also shown in the legend.

which are well studied in the experiments with synchrotron radiations [20] and radiations from a rare-gas discharge lamp [21]. Figure 5 of Ref. [20] shows the relevant potential energy curves of OCS^+ . One can consider two scenarios: In scenario 1, tunnel ionization onto dissociative excited states takes place directly, which corresponds to the ionization of $\text{HOMO} - n$. In scenario 2, tunnel ionization onto the ground X state of OCS^+ takes place first, and then multiphoton excitation onto dissociative excited states follows.

We first examine the possibility of scenario 1. As a rough estimate, we compare the experimental production rate of the specific fragment ion p_{frag} with that predicted by the ADK theory [22]. For the experimental value, we take the ratio of the number of the specific fragment ions to that of OCS^+ ions. For the theoretical value, we take the ratio of the ionization rate on the A, B, and C state of the OCS^+ to that on the X state of OCS^+ . In fact, it is reported that both the A and B states contribute to the production of S^+ , while the C state contributes to the production of both S^+ and CO^+ fragment ions [21]. On the other hand, CS^+ ions are produced via even higher states of OCS^+ [21], resulting in even lower ionization rates. We find that the experimental production rates of the specific fragment ions are much higher than those predicted

by the ADK theory [23], meaning that scenario 1 is very unlikely. Therefore, scenario 2 is more plausible, suggesting that multiphoton excitation from the ground state of OCS^+ to dissociative excited states takes place. From the viewpoint of tunnel ionization and considering the HOMO of an OCS molecule, our results for the dissociation channels producing S^+ , CO^+ , and CS^+ are consistent with the result reported in Ref. [8]. That is to say the ionization rate is higher when the electric field points toward the S atom.

Next we consider the laser intensity dependence of the asymmetry parameter $A_{\text{MF-PAD}}$ [especially for the S^+ channel (I)] based on the published information [24]. It is natural to think that in the intensity regime lower than $\sim 5 \times 10^{13} \text{ W/cm}^2$, the first excited A state contributes to the production of S^+ , while in the higher intensity regime, the B and C states start to contribute to the production of S^+ , CO^+ , and CS^+ . Since the decay times of the $\text{A}(^2\Pi_{3/2})$ and $\text{A}(^2\Pi_{1/2})$ are 110 and 80 ns [24], respectively, and are much longer than the rotational period (82 ps) of OCS molecules, the molecules can rotate many times during the dissociation along the $\text{A}(^2\Pi_{3/2})$ and $\text{A}(^2\Pi_{1/2})$ states. Consequently, the photoelectron angular distributions cannot be reflected in the MF-PADs in the lower intensity regime. On the other hand, since the MF-PADs correlated with S^+ , CO^+ , and CS^+ fragments have clear asymmetry in the higher intensity regime as shown in Fig. 5, the decay times of the B and/or C states, which are unknown, are expected to be shorter than the rotational period (82 ps) of OCS molecules.

Then we consider the dissociation channel $\text{OCS}^+ \rightarrow \text{O}^+ + \text{CS}$, for which the orientation dependence of the dissociative ionization is different from that for other channels (I), (II), and (III). Since the orbital shapes and the Stark shifts of HOMO-1 and HOMO-2 are different from those of HOMO, the observed orientation dependence for the O^+ channel may suggest the tunnel ionization from HOMO-1, HOMO-2, etc., which is actually consistent with our observation that the production ratio of the $\text{O}^+ + \text{CS}$ channel is the smallest among the four dissociative ionization channels studied here at the lower intensity of $5 \times 10^{13} \text{ W/cm}^2$, but it becomes the second at the higher intensity of $2.4 \times 10^{14} \text{ W/cm}^2$ [23].

Finally we discuss future subjects. Theorists are encouraged to develop an appropriate theoretical model of dissociative tunnel ionization which can be used to predict photoelectron angular distributions from polar polyatomic molecules depending on a specific dissociative ionization channel. Employing longer-wavelength ionization pulses, which better satisfy the tunnel ionization condition, should be interesting and important to investigating the scaling law in the orientation dependence in multichannel dissociative ionizations of OCS molecules. Few-cycle pulses will make the dissociation process simpler because the multiphoton excitation after tunnel ionization can be suppressed. Then the degrees of asymmetry $A_{\text{MF-PAD}}$ in MF-PADs shown in Fig. 5 may be accordingly suppressed if scenario 2 discussed above is the dissociation mechanism of OCS^+ cations for the channels (I), (II), and (III).

In conclusion, we have observed MF-PADs correlated with different dissociative ionization channels: $\text{OCS}^+ \rightarrow \text{S}^+ + \text{CO}$, $\text{CO}^+ + \text{S}$, $\text{CS}^+ + \text{O}$, and $\text{O}^+ + \text{CS}$. We find that the OCS molecules are more likely to be ionized when the electric field points toward the O atom for the dissociation channel leading to the production of O^+ , while they are more likely to be ionized when the electric field points toward the S atom for other dissociation channels. If we follow the tunnel ionization picture in the long-wavelength limit, the OCS molecules are more likely to be ionized from the S site for the dissociation channel leading to the production of O^+ , while they are more likely to be ionized from the O site for other dissociation channels.

The authors are grateful to Prof. A. Yagishita for his support in the development of our CO-VIS apparatus. We thank Dr. R. Yamashiro for his contribution in the early stage of the development of our CO-VIS apparatus. We also appreciate the assistance given by Dr. K. Kato and Mr. Y. Iida in the present study. This work was supported by Grants-in-Aid for Specially Promoted Research Grant No. 21000003 from MEXT, for Scientific Research (A) Grant No. 26247065 from JSPS, and for the Photon Frontier Network Program of MEXT. Y.S. is grateful for the financial support from Grant-in-Aid for JSPS Research Fellow, Grant No. 13J10603.

-
- [1] T. Kanai, S. Minemoto, and H. Sakai, *Nature (London)* **435**, 470 (2005).
- [2] K. Kato, S. Minemoto, Y. Sakemi, and H. Sakai, *Phys. Rev. A* **90**, 063403 (2014).
- [3] P. Agostini, F. Fabre, G. Mainfray, G. Petite, and N. K. Rahman, *Phys. Rev. Lett.* **42**, 1127 (1979).
- [4] T. Zuo, A. D. Bandrauk, and P. B. Corkum, *Chem. Phys. Lett.* **259**, 313 (1996).
- [5] H. Sakai, J. J. Larsen, I. Wendt-Larsen, J. Olesen, P. B. Corkum, and H. Stapelfeldt, *Phys. Rev. A* **67**, 063404 (2003).
- [6] X. M. Tong, Z. X. Zhao, and C. D. Lin, *Phys. Rev. A* **66**, 033402 (2002).
- [7] D. Pavičić, K. F. Lee, D. M. Rayner, P. B. Corkum, and D. M. Villeneuve, *Phys. Rev. Lett.* **98**, 243001 (2007).
- [8] L. Holmegaard, J. L. Hansen, L. Kalhøj, S. L. Kragh, H. Stapelfeldt, F. Filsinger, J. Küpper, G. Meijer, D. Dimitrovski, M. Abu-samha, C. P. J. Martiny, and L. B. Madsen, *Nat. Phys.* **6**, 428 (2010).
- [9] D. Dimitrovski, C. P. J. Martiny, and L. B. Madsen, *Phys. Rev. A* **82**, 053404 (2010).
- [10] D. Dimitrovski, M. Abu-samha, L. B. Madsen, F. Filsinger, G. Meijer, J. Küpper, L. Holmegaard, L. Kalhøj, J. H. Nielsen, and H. Stapelfeldt, *Phys. Rev. A* **83**, 023405 (2011).
- [11] M. Abu-samha and L. B. Madsen, *Phys. Rev. A* **82**, 043413 (2010).
- [12] O. I. Tolstikhin, T. Morishita, and L. B. Madsen, *Phys. Rev. A* **84**, 053423 (2011).
- [13] J. Wu, L. Ph. H. Schmidt, M. Kunitski, M. Meckel, S. Voss, H. Sann, H. Kim, T. Jahnke, A. Czasch, and R. Dörner, *Phys. Rev. Lett.* **108**, 183001 (2012).
- [14] H. Akagi, T. Otobe, A. Staudte, A. Shiner, F. Turner, R. Dörner, D. M. Villeneuve, and P. B. Corkum, *Science* **325**, 1364 (2009).
- [15] J. Svensmark, O. I. Tolstikhin, and L. B. Madsen, *Phys. Rev. A* **93**, 053426 (2016).

- [16] P. Eckle, M. Smolarski, Ph. Schlup, J. Biegert, A. Staudte, M. Schöffler, H. G. Muller, R. Dörner, and U. Keller, *Nat. Phys.* **4**, 565 (2008).
- [17] A. Staudte, S. Patchkovskii, D. Pavičić, H. Akagi, O. Smirnova, D. Zeidler, M. Meckel, D. M. Villeneuve, R. Dörner, M. Yu. Ivanov, and P. B. Corkum, *Phys. Rev. Lett.* **102**, 033004 (2009).
- [18] K. Hosaka, J. Adachi, A. V. Golovin, M. Takahashi, N. Watanabe, and A. Yagishita, *Jpn. J. Appl. Phys.* **45**, 1841 (2006).
- [19] U. Even, J. Jortner, D. Noy, N. Lavie, and C. Cossart-Magos, *J. Chem. Phys.* **112**, 8068 (2000).
- [20] M.-J. Hubin-Franskin, J. Delwiche, P.-M. Guyon, M. Richard-Viard, M. Lavollée, O. Dutuit, J.-M. Robbe, and J.-P. Flament, *Chem. Phys.* **209**, 143 (1996).
- [21] S. Morse, M. Takahashi, J. H. D. Eland, and L. Karlsson, *Int. J. Mass Spectrom.* **184**, 67 (1999).
- [22] M. V. Ammosov, N. B. Delone, and V. P. Kraĭnov, *Zh. Eksp. Teor. Fiz.* **91**, 2008 (1986) [*Sov. Phys. JETP* **64**, 1191 (1986)].
- [23] See Supplemental Material at <http://link.aps.org/supplemental/10.1103/PhysRevA.96.011401> for the comparison between the experimental production rate of the specific fragment ion p_{frag} of OCS^+ and that predicted by the ADK theory as a function of the intensity of the ionization pulse.
- [24] U. Bosel, R. Weinkauff, C. Weickhardt, and E. W. Schlag, *Int. J. Mass Spectrom. Ion Process.* **131**, 87 (1994).